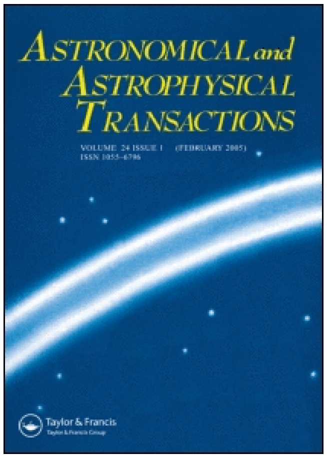

Astronomical & Astrophysical Transactions
The Journal of the Eurasian Astronomical Society
Publication details, including instructions for authors and subscription information:
http://www.informaworld.com/smpp/title~content=t713453505

Some H II region observations in **J** = 1 → 0 and 2 → 1 lines of $C^{18}O$

A. G. Kislyakov [a]; B. E. Turner [b]
[a] State University at Nizhny Novgorod, Russia
[b] National Radio Astronomy Observatory, USA

Online Publication Date: 01 November 1996
To cite this Article: Kislyakov, A. G. and Turner, B. E. (1996) 'Some H II region observations in **J** = 1 → 0 and 2 → 1 lines of $C^{18}O$', Astronomical & Astrophysical Transactions, 11:3, 279 - 285
To link to this article: DOI: 10.1080/10556799608205476
URL: http://dx.doi.org/10.1080/10556799608205476

Astronomical and Astrophysical Transactions, 1996,
Vol. 11, pp. 279–285
Reprints available directly from the publisher
Photocopying permitted by license only

SOME H II REGION OBSERVATIONS IN $J = 1 \rightarrow 0$ AND $2 \rightarrow 1$ LINES OF $C^{18}O$

A. G. KISLYAKOV[1] and B. E. TURNER[2]

[1] *State University at Nizhny Novgorod, Russia*
[2] *National Radio Astronomy Observatory, USA*

(Received March 3, 1995)

About 30 H II regions were observed in $C^{18}O$ lines. A $J = 1 \rightarrow 0$ line emission was detected in 24 zones while the $2 \rightarrow 1$ line emission – in 12 objects only. Radiative transfer equation has been solved for all 24 cases using LVG approximation. $C^{18}O$ column densities and hydrogen number densities of 12 clouds have been explored as the functions of Galaxy radius. Both quantities reveal no evident trend. Hydrogen number density does not vary significantly from cloud to cloud (with one exception of very rarefied object – BFS 54), while the cloud size-linewidth dependence corresponds to the subsonic Kolmogorov law.

KEY WORDS Galaxy structure, interstellar medium, H II regions, CO clouds, rotational lines

An HCN $J = 1 \rightarrow 0$ survey has been conducted [1] of about 100 Sharpless H II regions for molecular cloud cores investigation. Excitation of the HCN line requires two order greater gas density than that necessary for the CO $J = 1 \rightarrow 0$ line. Figure 1 presents the number of H II zones $N_1 = N(\mathrm{CO})$, whose $J = 1 \rightarrow 0$ radiation temperatures exceed 10 K, versus the galactocentric distance R. The $N_1(R)$ curve shows a maximum near $R \sim 10$ kpc, corresponding to the adopted Sun's distance from the Galaxy center. Hence, the $N_1(R)$ curve reflects an increasing difficulties in H II region detection as their distance from the Earth increases. The number of H II regions $N_2(\mathrm{HCN})$ exhibiting the HCN $J = 1 \rightarrow 0$ radiation temperature large than 1 K behaves analogously along R. However, the ratio N_2/N_1, free of selection effects, is decreasing as R increases (see Figure 1). This dependence can be a consequence of the gas density and temperature decreasing as R increases. According to the above mentioned objectives, the investigation of molecular cloud core density along galactic radius is very important. This paper presents the $C^{18}O$ $J = 1 \rightarrow 0$ and $2 \rightarrow 1$ line observations of a subset of molecular clouds in directions of H II zones. The following selection rules were adopted: (1) the H II region should be compact (optical radius $\leq 5'$); (2) its CO $J = 1 \rightarrow 0$ line should be single and symmetric and (3) the appropriate galactocentric distance of H II region. The objects to be observed were selected from papers [2, 3]. Their data were corrected later according to some recent publications. As can be shown [4], the CO $J = 1 \rightarrow 0$

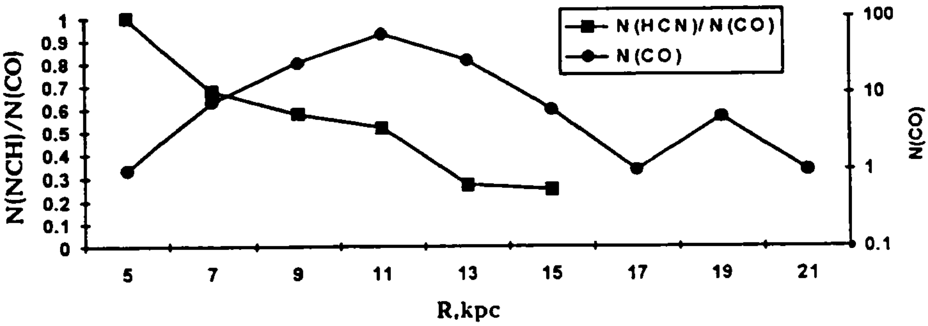

Figure 1 CO and HCN emissivities versus galactocentric distance.

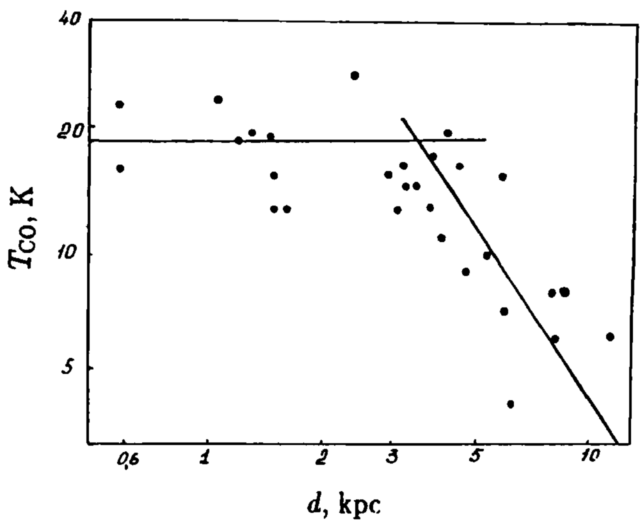

Figure 2 The CO cloud radiation temperatures as dependent on d

radiation temperature depends on molecular cloud distance from the Sun, d. Figure 2 gives an impression on $T_{CO}(d)$ function for a selected subset of the clouds. The dependence $T_{CO}(d)$ can be explained as caused by dilution effect owing to the cloud fragmentation. It yields the fragment size of about 2–2.5 pc.

The observations were conducted in November–December, 1991, using the NRAO† 12-meter radiotelescope at Kitt Peak (USA). Two dual polarization SIS receivers were employed with the system temperature ranging in 200–450 K ($J = 1 \to 0$, $\sim$ 109.8 GHz) and 800-2000 K ($J = 2 \to 1$, $\sim$ 219.6 GHz) as dependent on the weather conditions during observations. Two filter banks, 512 channels each,with the frequency resolutions of 100 and 250 kHz, were used in a parallel

†National Radio Astronomy Observatory is operated by Associated Universities under agreenment with National Science Foundation

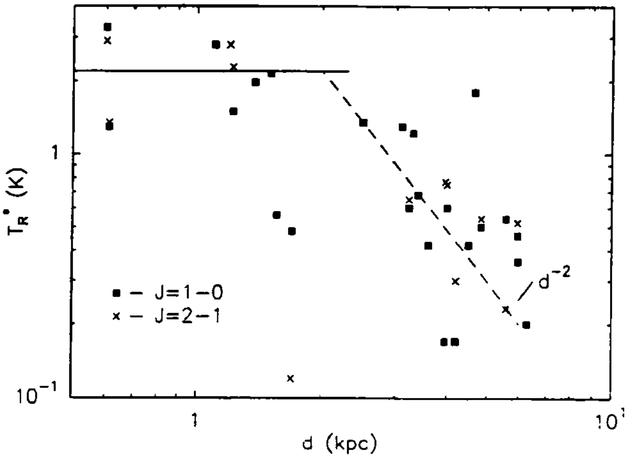

Figure 3 $C^{18}O$ radiation temperatures versus d. The $J = 1 \rightarrow 0$ data are denoted by squares and the $2 \rightarrow 1$ data by crosses.

mode. Very few spectra were taken with a greater resolution of 30 kHz. The observations were made in a switching frequency mode. Together with two polarizations added, the frequency switching gives a signal-to-noise ratio improvement by a factor of 2.

The $C^{18}O$ $J = 1 \rightarrow 0$ line was detected in 24 objects from 28 objects observed [4]. Five point maps were made with the centrum positions corresponding to the T_{CO} maxima. Additional offsets were tried if necessary in order to determine the position of maximum intensity. In about 20 cases the emitting region sizes were determined reliably. It is worth to note a good correlation between radio and optical sizes (correlation coefficient amounts to 0.88). CO and $C^{18}O$ peak positions as a rule do not coincide. That is natural if we take into account the difference in angular resolution. Nevertheless, the T_{CO} and $T_R^*(C^{18}O)$ $J = 1 \rightarrow 0$ radiation temperatures are well correlated (correlation coefficient is about 0.88). The accuracy of $T_{10} = T_R^*(J = 1 \rightarrow 0)$ values ranges in 0.025–0.055 K as dependent on T_{sys} during observations. Figure 3 presents the T_{10} data as function of d. The $T_{10}(d)$ dependence can be interpreted as previously, leading to the typical fragment size of $\sim$ 0.6 pc, significantly less than in the preceeding case. The $T_{10}(R)$ function (it was discussed in [5]) is similar to T_{CO} from Figure 1. Note the above mentioned good correlation of T_{10} and T_{CO}.

The linewidth – cloud size $\Delta V(D)$ relation is crucial from the point of view of cloud kinematics [6]. The linewidths meausered at the positions of emission maximum are plotted on Figure 4 versus the mean diameter of the cloud. The $\Delta V(D)$ dependence can be presented in a logarithmic scale by

$$\log\left[\frac{\Delta V}{\mathrm{km/s}}\right] = \log\left\{(0.9 \pm 0.03)\left[\frac{D}{\mathrm{pc}}\right]^{(0.31\pm0.04)}\right\}, \tag{1}$$

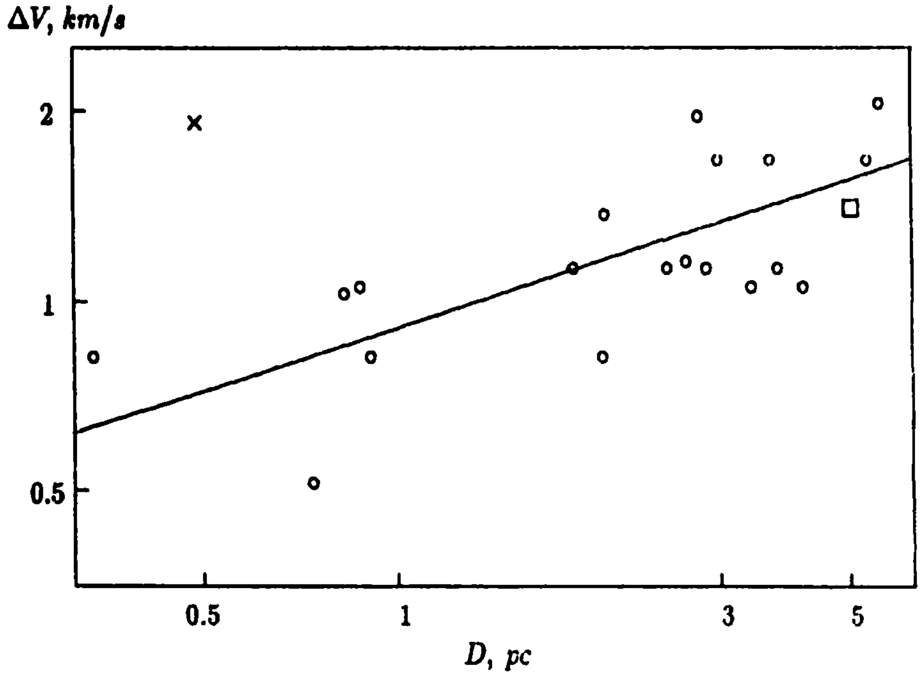

Figure 4 The linewidth-cloud size dependence. Data for two clouds are indicated by cross (S 106) and box (the S 201 envelope parameters from [9]).

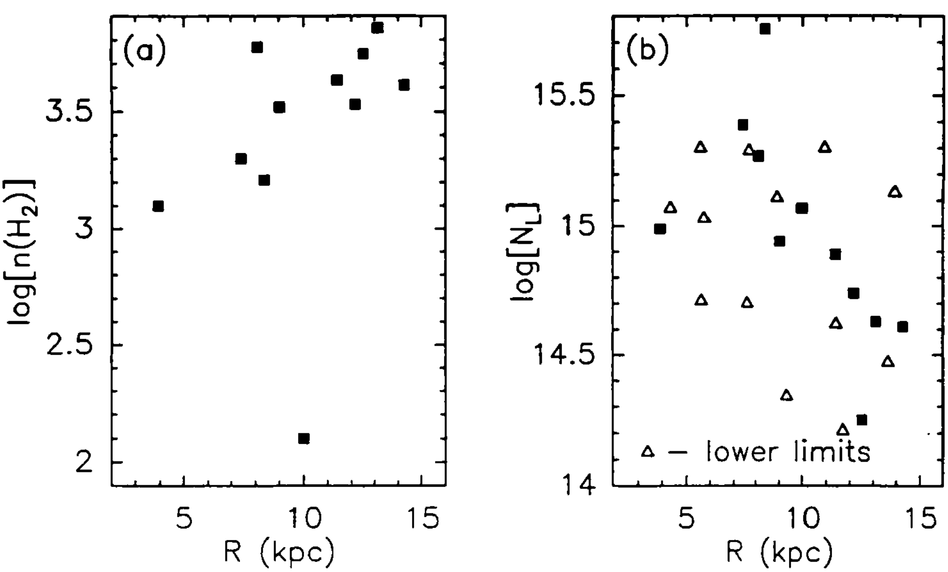

Figure 5 *a*, The hydrogen number density of the clouds; *b*, $C^{18}O$ column density of the clouds.

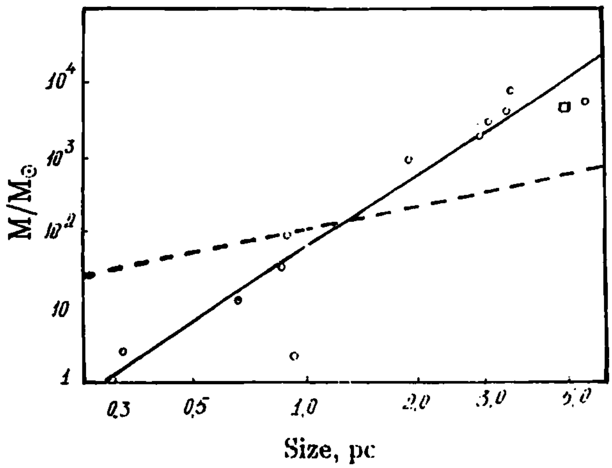

Figure 6 The cloud core mass as dependent on the cloud core size. The S201 envelope data are presented by box.

found by the least-mean-squares method. Equation (1) parameters are analogous to the well known data on molecular clouds (see, for instance, [6]). Surprizingly, there is a good correlation in CO and $C^{18}O$ line widths for this population (correlation coefficient is of 0.82).

Every attempt to detect the $C^{18}O$ $J = 2 \rightarrow 1$ line was successful. These results are summarized in the Figure 3 as well. The $T^*_R(J = 2 \rightarrow 1) = T_{21}$ radiation temperatures were measured as a rule at the points of emission maxima determined in the $J = 1 \rightarrow 0$ line. There is one exception to the rule, the S201 source which is discussed in [7, 8]. The radiation temperatures T_{10} and T_{21} are perfectly correlated (correlation coefficient equals to 0.977), see also [5]. The T_{21} values evidently depend on d as well (see Figure 3). Thus, the $T^*_R(d)$ dependence can be seen from the data obtained at different frequencies and with different angular resolutions. It puts some constraints on the possible models explaining the $T^*_R(d)$ dependence.

Using data for the two transitions one can solve the radiative transfer equation for a cloud and determine its density for a given kinetic temperature. The kinetic temperatures can be found from CO data, the maximum observed values were adopted. The radiative transfer equation has been solved assuming the LVC-model. The calculated cloud core densities n_{H_2} and $C^{18}O$ column densities N_1 are presented in Figure 5 (a, b) as function of R. As it can be seen from these figures, both n_{H_2} and N_1 do not show clear systematic trend as galactocentric distance grows. The core densities range within $(1\text{–}7)10^3$ cm^{-3} with the mean value of 4×10^3 cm^{-3}. The only exception is the anomalously rarefied object S54 with $n_{H_2} = 1.2 \times 10^2$ cm^{-3}. Figure 6 compiles the cloud core masses. We estimate the rms errors in n_{H_2} and D to be as high as $\pm 20\%$ and $\pm(10\text{–}15)\%$, respectively. Thus, the total rms error in mass should not exceed significantly $\pm(30\text{–}35)\%$. The size-mass dependence for cloud cores is very essential as regards their state and evolution. The experimental points in Figure 6 can be approximated by

$$\log\left[\frac{M}{M_\odot}\right] = \log\left\{(56^{+24}_{-16})\left[\frac{D}{\mathrm{pc}}\right]^{(3.2\pm0.3)}\right\}. \tag{2}$$

Equation (2) was obtained using least mean squares method. Obviously, the H II region molecular clouds form a population with the global distribution different from that of molecular clouds in total. Molecular clouds with developed star formation can evidently differ in their physical properties from those at initial stages. Our results support these considerations. For example, the CO $J = 1 \rightarrow 0$ surveys lead to the linewidth-cloud size law [10] $\Delta V \propto D^{0.5}$ km/s. That is typical for clouds prior to gravitational instability and subject to constant external pressure. Our observations give $\Delta V \propto D^{0.31}$ in accordance with the law of subsonic Kolmogoroff turbulence. Note, that CO $J = 1 \rightarrow 0$ data for the same population of molecular clouds give a similar dependence

$$\Delta V = (1.5 \pm 0.1)D^{(0.29\pm0.05)}\ \mathrm{km/s}.$$

That is a sequence of CO and $C^{18}O$ linewidths good correlation implying insignificant saturation and blending effects of CO lines. Giant molecular clouds contain about 90% of interstellar gas in molecular form. Their sizes are ≥ 20 pc and masses $\geq 10^5 M_\odot$ [10]. The sizes and masses of cloud cores explored in this paper range within 0.3–5.5 pc and $(2.3 \div 7.8) \times 10^3 M_\odot$. It is natural, that the line saturation and blending effects are less prominent in such compact objects. These effects lead to the dependences $n_{H_2} \propto D^{-1}$ and $M \propto D^2$. As follows from the preceeding section, the mean density of the cloud cores does not depend on their size while $M \propto D^3$.

We assess the $T_{CO}(d)$ and $T_{10}(d)$ dependences as the sequence of dilution owing to clouds fragmentation. Note that the whole population of the clouds associated with H II zones [3] demonstrates the same dependence $T_{CO}(d)$ leading to the fragment size of ~ 2.8 pc. Our set of clouds gives the fragment size of 2–2.5 pc, considerably exceeding that determined from the T_{10} dependence: ~ 0.6 pc. The latter value is close to the minimal measured size of a cloud core.

The state of the cloud, as regards to the virial equilibrium, depends on its fragmentation as well. The dashed line in Figure 6 gives the virial mass for $T_k = 20$ K. As follows from Figure 6, the clouds with $D \leq 1$ pc can be gravitationally unstable. However, fragmentation of a cloud makes it stable, because the reasons that caused the fragmentation can prevent the instability as well. The mean density of cloud cores as determined from $C^{18}O$ observations amounts to $\sim 4 \times 10^3$ cm^{-3}, considerably less than the core density established from HCN and HCO^+ observations [10]. It is natural because excitation of these molecules requires about two-order higher density than that for CO. HCN and HCO^+ cloud cores are more compact, 0.15–3 pc. The largest cores can exceed the virial mass as well. Note that the HCN observations give some more arguments in favor of cloud fragmentation [10].

Thus, the density of cloud cores does not show systematic variation as the galactocentric distance of a cloud increases from 4 to 14 kpc. Concerning the detected trend in HCN emission [1], the dilution effect or HCN abundance variation seem to be more plausible explanations than the cloud density decreasing as R increases.

Acknowledgements

One of the authors (AGK) is very greatful to the NRAO for generous support. His work was partly supported also with ESO grant A-02-001 and RFFR grant 95-02-87413.

References

1. Burov, A. V., Zinchenko, I. I., Kislyakov, A. G. *et al.* (1988) *Pis'ma v AZh* **14**, No. 3.
2. Blitz, L., Fich, M., Stark, A. A. (1982) *Ap. J. Suppl. S.* **49**, 183.
3. Fich, M., Blitz, L. (1984) *Ap. J.* **279**, 125.
4. Kislyakov, A. G. and Turner, B. E. (1995) *Astron Zh.* **72**, 168.
5. Kislyakov, A. G. and Turner, B. E. (1993) *First Eurasian Symp. on Space Sci. & Techn.*, Gebze., Turkey, (1994) *Turk. J. of Phys.* **18**, 987–991.
6. Fuller, G. A., Myers, P. C. (1991) *Center for Ap. Prep. Ser.* No. 3282.
7. Kislyakov, A. G. and Turner, B. E. (1994) *Pisma v AZh* **20**, 822–826.
8. Kislyakov, A. G. and Turner, B. E. (1996) This Issue.
9. Combes, F. (1991) *Ann. Rev. A& A* **29**, 195.
10. Zinchenko, I. I. (1992) *A&A Trans.*, No. 1, 53.